

Magnetic Properties of CoFe_2O_4 nano particles hosted in Silica Xerogels

A Thesis Submitted in Partial Fulfillment of the
Requirements for the Degree of
Bachelor of Technology

By

PHIBAHUNLANG SWER

(Roll No: 10508018)



**DEPARTMENT OF CERAMIC ENGINEERING
NATIONAL INSTITUTE OF TECHNOLOGY, ROURKELA, ORISSA**

Magnetic Properties of CoFe_2O_4 nano particles hosted in Silica Xerogels

A Thesis Submitted in Partial Fulfillment of the
Requirements for the Degree of
Bachelor of Technology

By

PHIBAHUNLANG SWER

(Roll No: 10508018)

Under the guidance of

DR. JAPES BERA



**DEPARTMENT OF CERAMIC ENGINEERING
NATIONAL INSTITUTE OF TECHNOLOGY, ROURKELA, ORISSA**



**NATIONAL INSTITUTE OF TECHNOLOGY
ROURKELA 769008, INDIA**

Certificate of recommendation

This is certified that the work contained in the thesis entitled “ Magnetic Properties of CoFe₂O₄ Nanoparticles Hosted in Silica Xerogels” by Phibahunlang Swer has been carried out under my supervision and that this work has not been submitted elsewhere for a degree.

May 2009

J.Bera

Assistant Professor

Dept of Ceramic Engineering

National Institute Of Technology

Rourkela

ACKNOWLEDGEMENT

I would like to express my gratitude to all those who had been with me throughout my project. To start with I would like to thank my guide Dr.J.Bera for his able technical guidance without which the project work could not have been carried out. I would like to thank the other faculty member of the dept for their cooperation. I would also take this opportunity to thank J.P.Nayak whose help, stimulating suggestions and encouragement helped me in all the time of my project work and for writing of this thesis. I am grateful to all my friends who have constantly helped me, encouraged and have worked with me in completing this project.

Last but not the least I would thank the almighty God who gave me all the strength to carry my work with sincerity and honesty

PHIBAHUNLANG SWER

CERAMIC ENGG

ROLL NO 10508018

ABSTRACT

CoFe₂O₄/SiO₂ magnetic nanocomposites have high potential for applications as magnetic fluids , drug delivery , and high density information storage due to the remarkable properties of bulk cobalt ferrite (strong anisotropy, high saturation magnetization and coercivity, mechanical hardness, and chemical stability), combined with the magnetic properties typical of the nanoparticles, which depend strongly on particle size and shape, particle–matrix interactions, and degree of dispersion throughout the matrix.

However, the aggregation and the coarseness of nanocrystallites at elevated temperature remain a critical obstacle for most of these synthesis techniques when fabricating the required nanoparticles. In order to overcome the obstacle, attempts have been made by dispersing nanoparticles in suitable matrix, such as resin, polymer films and silica glass. . Hence, it is a challenge to disperse nano particles completely and synthesized it by a simple processing. Therefore, a project has been taken up to study the magnetic properties of CoFe₂O₄ nanoparticles hosted in silica gel. The report presents the synthesis of CoFe₂O₄ nanoparticles hosted in silica xerogels and its characterization in terms of its particles size, effect of concentration on the magnetic properties.

CONTENTS OF THE THESIS

CONTENTS	PAGE
Background	1
Objective	5
Experimental	6
Preparation of silica xerogel from rice husk ash	6
Preparation of Cobalt Ferrite silica nano composite	6
Characterization	8
Results and Discussion	10
XRD	10
FTIR	12
Particle and Crystallite size measurement	14
Magnetic property	17
Conclusions	19
Reference	20

List of Figures

Fig. 1 Biomedical applications of magnetic NPs.	1
Fig. 2 Preparation of silicacoated magnetic nanocomposites. (i) Initial optional coating with sodium silicate; (ii) base catalysed condensation of TEOS on nanoparticle surface	3
Fig. 3 Flow chart of silica xerogel synthesis from rice husk.	7
Fig. 4 Flow chart of cobalt ferrite nanoparticle synthesis hosted in silica matrix.	8
Fig. 5 DSC/TG of Co-ferrite silica matrix	11
Fig. 6 XRD patterns of the Co-ferrite silica matrix samples calcined at different temperatures.	11
Fig. 7 (a) Co-ferrite silica matrix (without heat treatment)	13
Fig. 7 (b) Co-ferrite silica matrix heated at 600°C	13
Fig. 7 (c) Co-ferrite silica matrix heated at 900°C	14
Fig. 8(a) Particle size distribution of silica coated Co-ferrite	15
Fig. 8 (b) XRD patterns of the Co-ferrite hosted in silica xerogels	15
Fig. 8 (c) XRD patterns of the Co-ferrite silica matrix samples prepared by dipping the gel with different times in Co-Fe solution, calcined at 1000°C temperature.	16
Fig. 9 Magnetization curves for SiO ₂ /CoFe ₂ O ₄ composite with different molar concentration of CoFe ₂ O ₄ .	18

LIST OF TABLES

Table 1 Crystallite sizes of CoFe ₂ O ₄ hosted in silica matrix.	16
--	----

Background:

Because their properties differ from those of their bulk counterparts, nanoparticles offer a range of potential applications based on their unique characteristics. In particular, magnetic nanomaterials represent one of the most exciting prospects in current nanotechnology. Fig. 1 shows one of the most important applications of magnetic nanoparticles (NPs), i.e. biomedical applications.

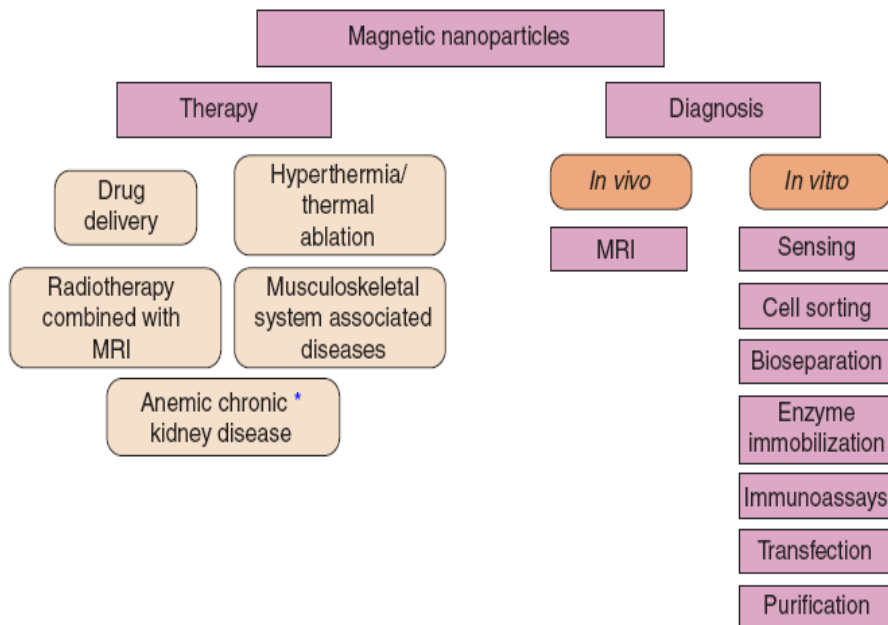


Fig. 1 Biomedical applications of magnetic NPs.

Nanocomposites consisting of nanoparticles dispersed in different matrixes have been a subject of extensive investigation in recent years. One motivation for the preparation of such nanocomposites is that they frequently possess unique properties. A well-known example is the superparamagnetism displayed by nanocomposites containing super paramagnetic nanoparticles dispersed into a nonmagnetic matrix. As a matrix material, silica has been the most widely researched and exploited. It is believed that nanocomposites of this type will become increasingly important for different applications for example, in magneto-optics, where they could be used for sensing [1], information storage [2] or optical insulation [3].

Nanocomposites with magnetic properties are also important in biomedicine, for example, for magnetic separation [4,5]. Moreover, large amounts of inexpensive magnetic particles are used

in the fields of environmental, chemical and biomolecular industrial separations and reactions [6, 7]. For applications involving high gradient magnetic separation, individual functionalized superparamagnetic nanoparticles are frequently not desired because they are too small to be efficiently captured. On the other hand, larger ferromagnetic particles can be easily separated from the mixture, but cannot be redispersed due to strong magnetic aggregation. A possible solution is to use submicron-sized superparamagnetic nanocomposite particles displaying high magnetizations.

Studies on nanocomposite magnetic materials, especially the core/shell structure magnetic materials, are of great interest for both fundamental magnetic investigation and engineering application. In fundamental studies, the coated nanoparticles are of interest as the shell layer prevents the nanoparticles from coarsening, surface oxidation and agglomeration. In soft magnetic application, nanocomposite materials composed of magnetic nanoparticles embedded in a dielectric matrix have attracted some research interest for their potential applications as microwave absorbing, shielding materials and electromagnetic devices [8–13].

Silica-coated Magnetic Nanoparticles have additional advantages. On the one hand, the external surface of silica coatings can be functionalized to allow the binding of biomolecules. This is mainly related to the presence of hydroxyl surface groups in significant concentrations that provide intrinsic hydrophilicity and allow surface attachment by covalent linkage of specific biomolecules. On the other hand, the internal porosity of silica can be used to host a specific drug, a feat achievable while avoiding the unwanted physical adsorption of larger molecules. Thirdly, the silica surface can be easily functionalised, enabling chemical bonding of various fluorescent and biological species to the surface. Another important aspect is that the silica coating may reduce any potential toxic effects of the bare nanoparticles. Silica and other microporous inorganic materials are heat resistant, with high surface areas and good mechanical strength

It also helps to prevent particle aggregation and increase their stability in solution. Because the isoelectric point of ferrite is about pH 7, it is necessary to further coat the particles in order to make them stable in the pH region 6–10. Application of a thin layer of silica lowers this isoelectric point to approximately pH 3, which increases the stability near neutral pH [14]. Finally silica coating has a significant advantage over traditional surfactant coating such as lauric

acid and oleic acid because there is no risk of desorption of the strongly covalently bound silica shells. There are a number of reports on the preparation of fluorescent-magnetic nanocomposites using a silica-coating approach. A general description is given in Fig. 2.

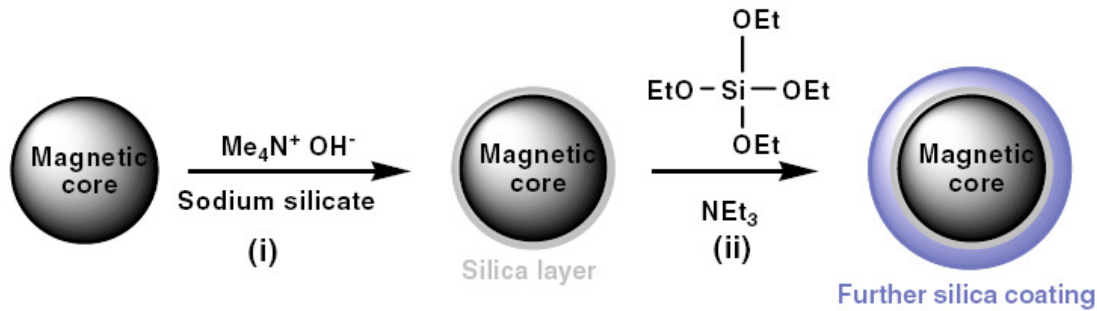


Fig. 2 Preparation of silicacoated magnetic nanocomposites. (i) Initial optional coating with sodium silicate; (ii) base catalysed condensation of TEOS on nanoparticle surface

$\text{CoFe}_2\text{O}_4\text{-SiO}_2$ magnetic nanocomposites have high potential for applications as magnetic fluids [15], drug delivery [16], and high density information storage [17] due to the remarkable properties of bulk cobalt ferrite (strong anisotropy, high saturation magnetization and coercivity, mechanical hardness, and chemical stability) [18], combined with the magnetic properties typical of the nanoparticles, which depend strongly on particle size and shape, particle–matrix interactions, and degree of dispersion throughout the matrix.

Based on the above technological challenge and scientific importance, researches such as sol–gel, micro-emulsion, templating, hydrothermal reaction, electrochemical synthesis, oxidative precipitation, citrate precursor method and sonochemical method [19-23] have been made into various synthesis routes of nanocrystalline ferrites. However, the aggregation and the coarseness of nanocrystallites at elevated temperature remain a critical obstacle for most of these synthesis techniques when fabricating the required nanoparticles. In order to overcome the obstacle, attempts have been made by dispersing nanoparticles in suitable matrix, such as resin [24], polymer films [25] and silica glass [26–28].

Moreover, most of these techniques require large amounts of organic liquids, expensive reagents (i.e. surfactants) or precursors, and complex preparation sequences. For high value added preparations such considerations are of little importance, but for large scale industrial applications (as the mass scale production of nanoparticle-based materials or manufacture of catalysts for environmental remediation or the synthesis of bulk chemicals) cost is a priority and therefore expensive procedures must be avoided, if possible.

Exotemplating techniques [29,30], consisting in the calcination of the oxide precursors within the pores of a rigid and porous template (i.e. active carbon [30,32] or silica gel [29,31,33–37]), which is later removed, have proven to be among the cheapest and easiest fabrication methods of high surface area oxides.

Objectives:

Objective of the present investigation were:

1. To synthesis CoFe_2O_4 nanoparticles hosted in silica xerogel.
2. To separate CoFe_2O_4 nanoparticles from silica host and its characterization.
3. To prepare sodium silica coated CoFe_2O_4 nanoparticles for its practical applications.

Experimental:

Preparation of silica xerogel from rice husk ash:

Silica xerogel, the host for CoFe_2O_4 nanoparticles, was prepared from rice husk ash (RHA). RHA was prepared from rice husk. Since rice husk comes along with many sand particles and other impurities, therefore it is necessary to clean it thoroughly. Cleaning of rice husk includes the air flow separation method; where air was blown and the sand and impurities being heavier were separated from the rice husk. Further cleaning was done by washing the rice husk with water. The Rice husk is then kept for drying in oven for about 8 hrs at 100°C . The dried rice husk was then burnt at 700°C for 6 hrs in a furnace. After complete combustion of rice husk, the husk turned into RHA. This RHA contains about 95 % silica.

The flow-chart for the silica xerogel synthesis is shown in Fig. 3. For a typical synthesis, about 5g of RHA added into 100 cc of 1 M NaOH solution and then boiled it for one hour with reflux condition. The boiled solution filtered by using Whatman 41 filter paper. The silica solution hence forward considered as Na_2SiO_3 solution. For the gel formation, drop wise addition of Na_2SiO_3 solution into 1N HCl solution, under continuous stirring was done on a magnetic stirrer until gel starts forming. The pH of this obtained wet gel was about 6. The gel was then kept for ageing for 1 day. Washing of the aged wet gel was done for 3 days with distilled water for about 10 times on each day. Washing was done so as to remove the sodium (Na^+) from the gel. After thoroughly washing the gel dried for 12 hrs at 110°C .

Preparation of Cobalt Ferrite silica nano composite:

The flow-chart for CoFe_2O_4 nanoparticle synthesis hosted in silica xerogel is shown in Fig. 4. Raw materials used for this preparation are silica gel as prepared, iron nitrate [$\text{Fe}(\text{NO}_3)_3 \cdot 9\text{H}_2\text{O}$], cobalt nitrate [$\text{Co}(\text{NO}_3)_2 \cdot 6\text{H}_2\text{O}$]. Iron nitrate [$\text{Fe}(\text{NO}_3)_3 \cdot 9\text{H}_2\text{O}$] along with cobalt nitrate $\text{Co}(\text{NO}_3)_2 \cdot 6\text{H}_2\text{O}$ was taken in a ratio of 2:1. After the solution was prepared, silica gel was impregnated and was kept for soaking for 24hrs. The solution obtained was then filtered and dried at about 110°C and weighed. The sample obtained changed its colour to deep orange/yellow and after heating its colour changed to amber. This heated sample obtained was again dipped in the same solution of cobalt ferrite (CoFe_2O_4) and repeated procedure was

followed. The sample was calcined at different temperature from 200 to 1000°C for different analysis purpose.

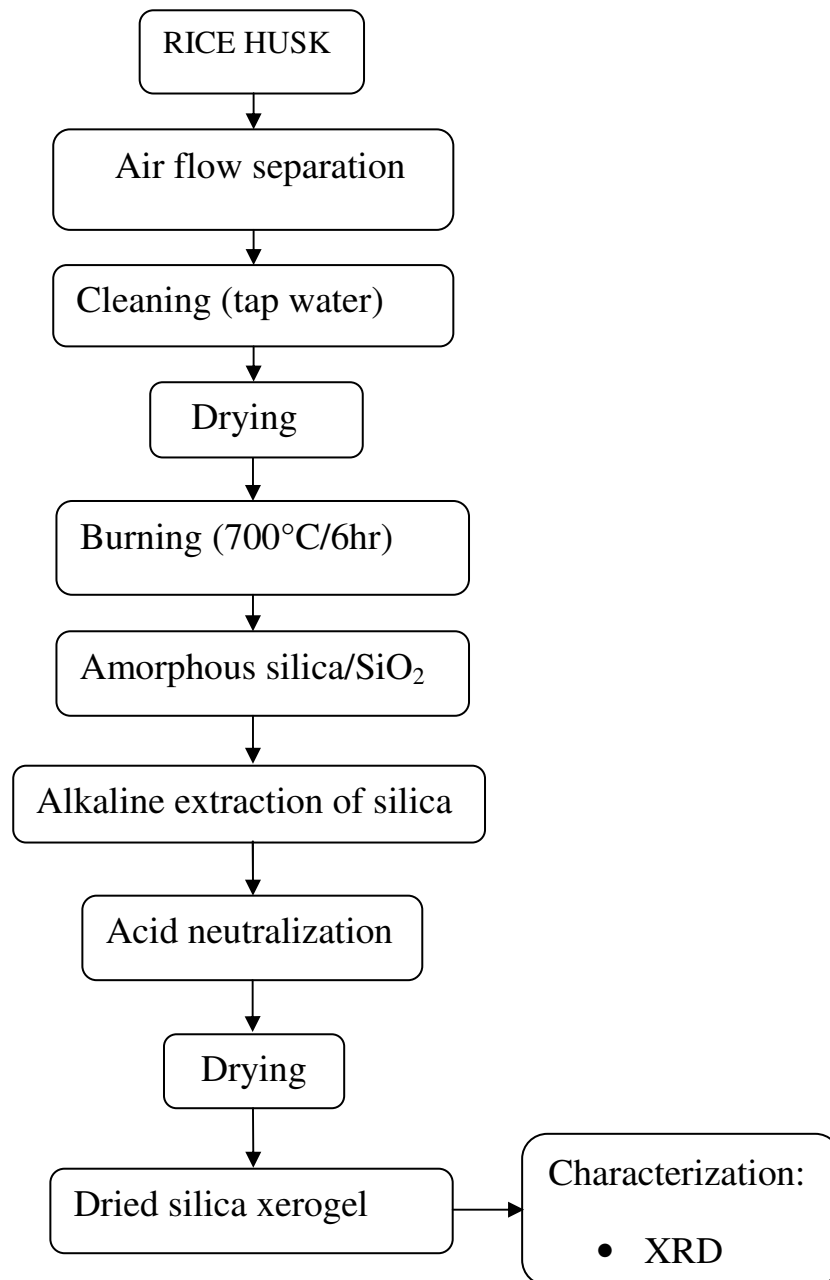


Fig. 3 Flow chart of silica xerogel synthesis from rice husk.

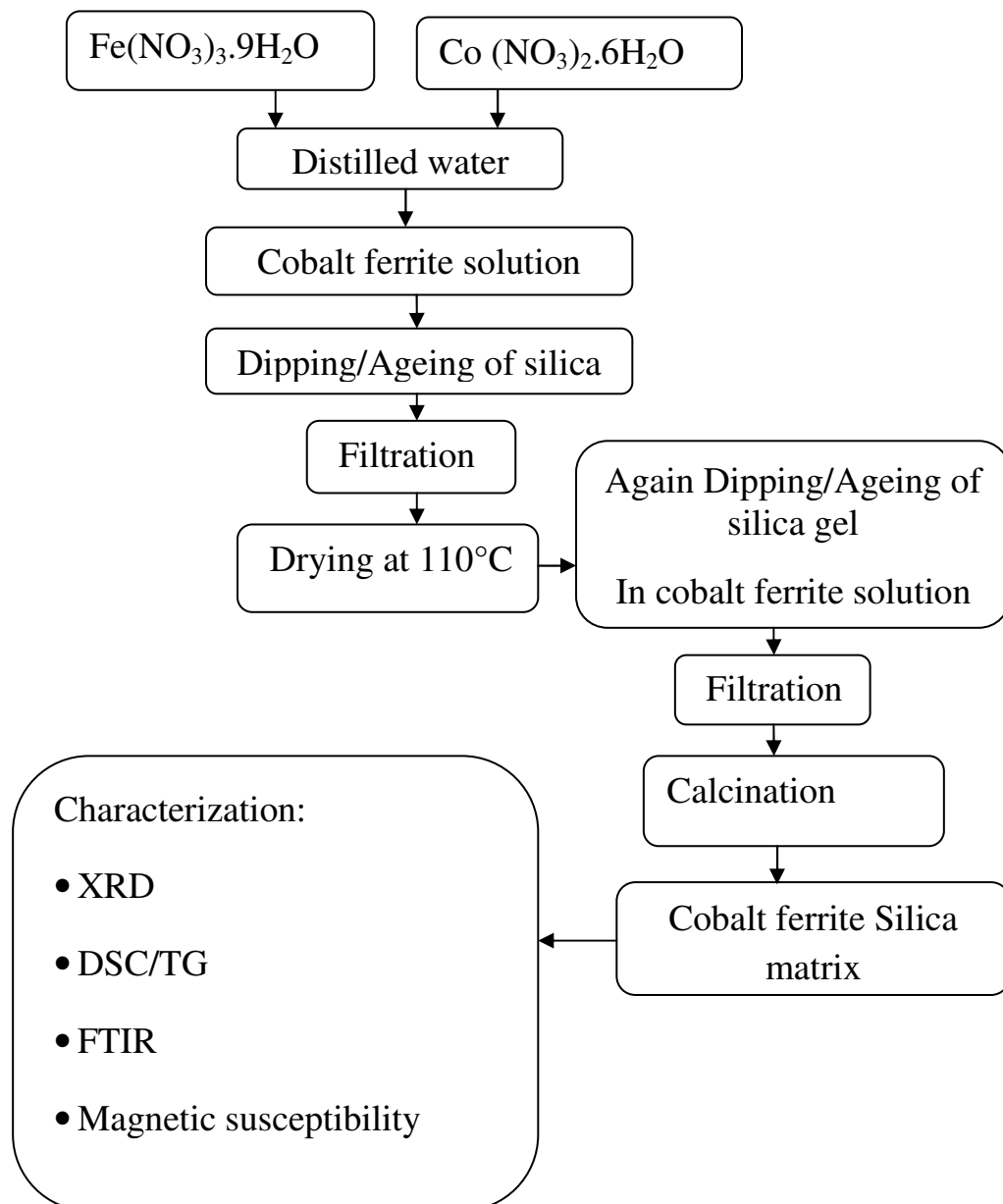


Fig. 4 Flow chart of cobalt ferrite nanoparticle synthesis hosted in silica matrix.

Characterization:

Thermal behaviors of the samples were carried out in N₂ atmosphere at a heating rate of 10°C/min, using DSC/TG, Netsch STA 449 C Jupiter thermal analysis system. The CoFe₂O₄/SiO₂ nano-composites were characterized for phases using a powder X-ray diffractometer (Philips PW1830 Holland). The IR spectra (FTIR, Spectrum RX-1, Perkin Elmer),

from 4000 to 400 cm^{-1} , were recorded by using pellets obtained dispersing the samples in KBr. The average crystallite diameters (DXRD) were calculated from the X-ray peak broadening of the diffraction peak using Scherer's formula. Nano particle size analyzer (Malvern, nano series) was employed for studies of particle size of cobalt ferrite in silica. The hysteresis loops of the nanocomposites were collected using a vibrating sample magnetometer with a maximum applied magnetic field of 20 KOe. M_s values at room temperature were obtained by extrapolation to infinite field in M versus $1/H^2$ plot.

Results and Discussion:

The TG-DSC curve measured in N₂ atmosphere for the silica xerogel is shown in Fig. 5. The strong endothermic peak at 110°C was related to the evaporation of H₂O. The small exothermic peak at 230°C was probably associated with the combustion of the organic compound. The very small exothermic hump at 580°C probably attributed to the complete decomposition. Another small exothermic hump at 850°C might be due to crystallization of CoFe₂O₄ phase. A possible explanation for small exothermic peak was that the combustion process of the NO₃⁻ ions overlapped the nucleation process for CoFe₂O₄ clusters, and the thermal energy released during the former process further promoted the latter process. Weight loss was extensive up to 150°C, and then continued gradually up to 600–800°C with the rate of loss in weight diminishing with the increase in temperature.

XRD:

Fig. 6 shows the XRD patterns of the Co-ferrite silica samples with molar ratio 1:3 (57 wt.% of Co-ferrite) dried at 110°C and then calcined at 400, 600, 800, 1000°C, respectively. The results demonstrate that the xerogel obtained after drying at 110°C is amorphous, no crystal phase is detectable. The XRD spectra of the samples reveal that weak peaks assigned to CoFe₂O₄ appear at 400°C, suggesting that particles of CoFe₂O₄ have nucleated in the silica matrix. The characteristic peaks of CoFe₂O₄ increase in intensity with increasing temperature of the calcinations treatment. The formation of the cobalt ferrite phase is nearly completed at 800°C. No diffraction lines of other phases can be observed.

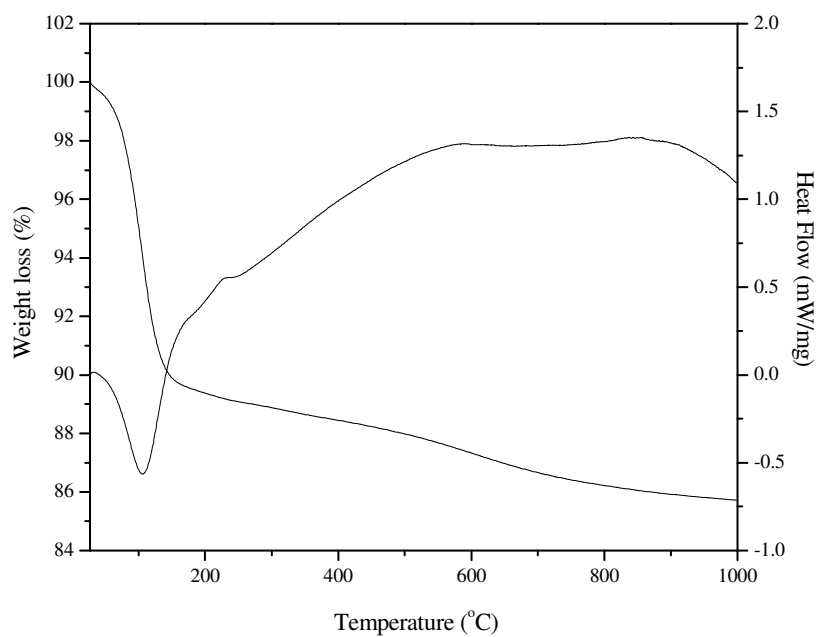


Fig. 5 DSC/TG of Co-ferrite silica matrix.

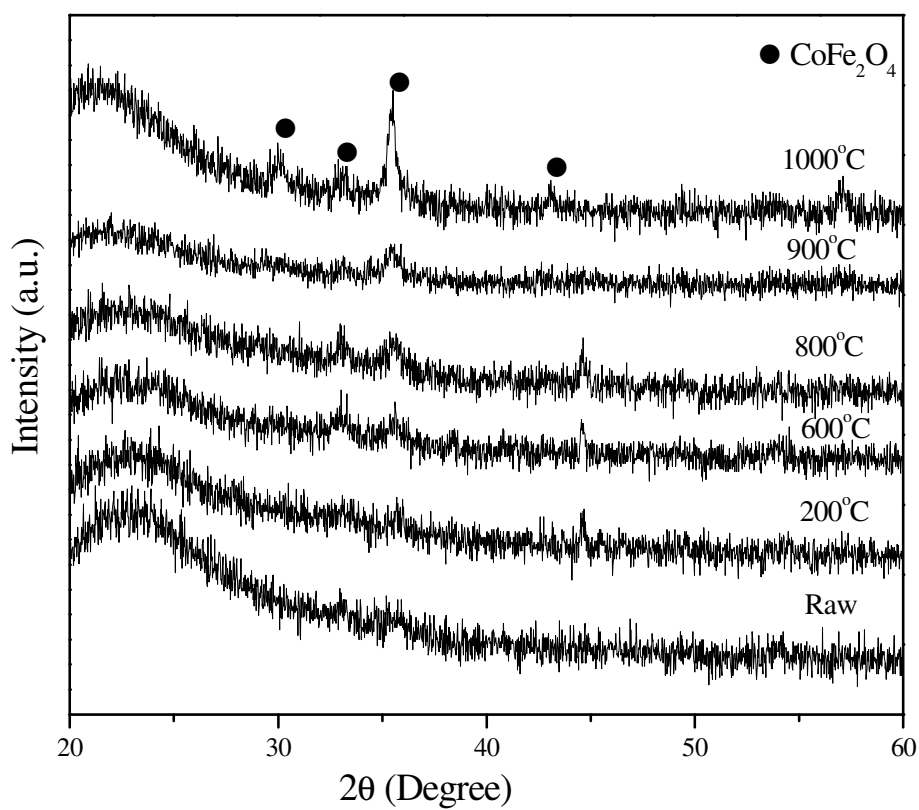


Fig. 6 XRD patterns of the Co-ferrite silica matrix samples calcined at different temperatures.

FTIR:

The changes in the matrix microstructure and the pore environment before and after heat treatment at various temperatures were followed by IR spectroscopy on the $\text{CoFe}_2\text{O}_4/\text{SiO}_2$ nanocomposites shown in Fig. 7 (a-c). For the Co-ferrite silica gel, without heat treatment, the broad band centered at 1637.56 cm^{-1} was assigned to the H–O–H bending vibration of the absorbed water. Obviously, there are certain amounts of microspores that exist in the present xerogel, which must contain physical absorbed water molecules. Strong absorptions at 1097.50 , 796.60 and 468.70 cm^{-1} indicate the formation of silica network. The band at 860.09 cm^{-1} is assigned to Si–O–Fe. The presence of Si–O–Fe vibrations reflects some interaction between the highly isolated Fe^{3+} ions and the nearest silica matrix. The presence of Si–O–Fe and Co–O bonds sufficiently reflects the chemical nature of the transition metals involved in the xerogel. That is, these transition metal ions do not participate directly in the sol–gel chemistry even though they were introduced into the starting solutions in the form of soluble inorganic salts. For the samples obtained at a treatment temperature of 600°C , the absorption band at 1079 cm^{-1} for $\equiv\text{Si–O–Si}\equiv$ of the SiO_4 tetrahedron is further broadened, while that for Si–O–Si or O–Si–O bending mode at 468 cm^{-1} is much weaker, which corresponds to a rearrangement process of silica network. Correspondingly, the absorption of the Fe–O stretching band in Fe–O–Si bonds increases in intensity. These facts reflect the formation of CoFe_2O_4 clusters that is accompanied with the rearrangement of silica network and with the enhancement of the Si–O–Fe bonds between the CoFe_2O_4 clusters and the surrounding silica network. For samples heat treated at 900°C , the IR spectrum changes greatly compared with that for samples heat treated at 600°C . The absorption at 1095 cm^{-1} for $\equiv\text{Si–O–Si}\equiv$ of the SiO_4 tetrahedron grows narrower and stronger, while the band at 970 cm^{-1} was disappeared. The breakage of the Fe–O–Si bonds in the interface between the clusters and matrix and the formation of CoFe_2O_4 clusters are probably results of the transformation from FeO_6 octahedron to FeO_4 tetrahedron.

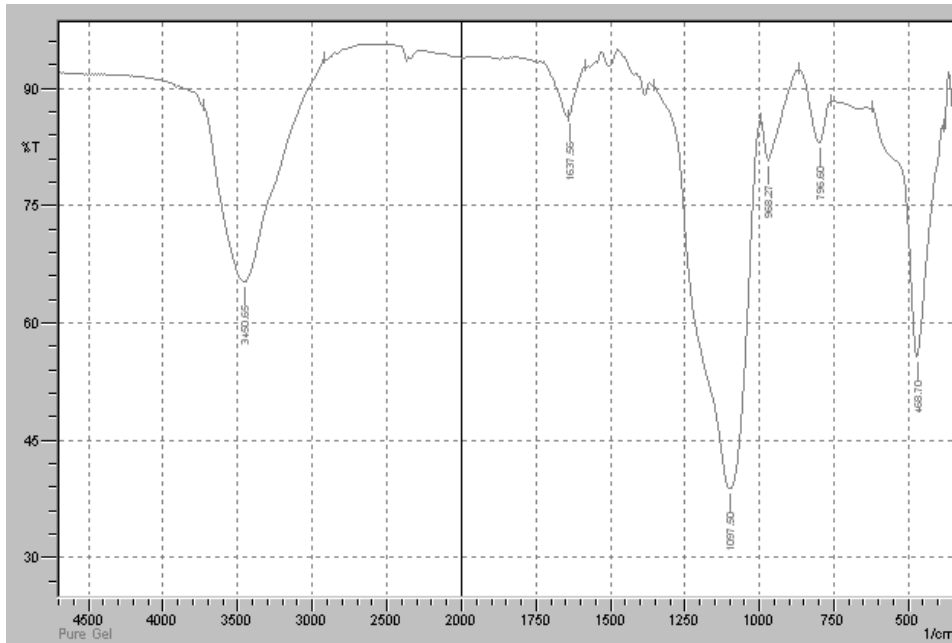


Fig. 7 (a) Co-ferrite silica matrix (without heat treatment)

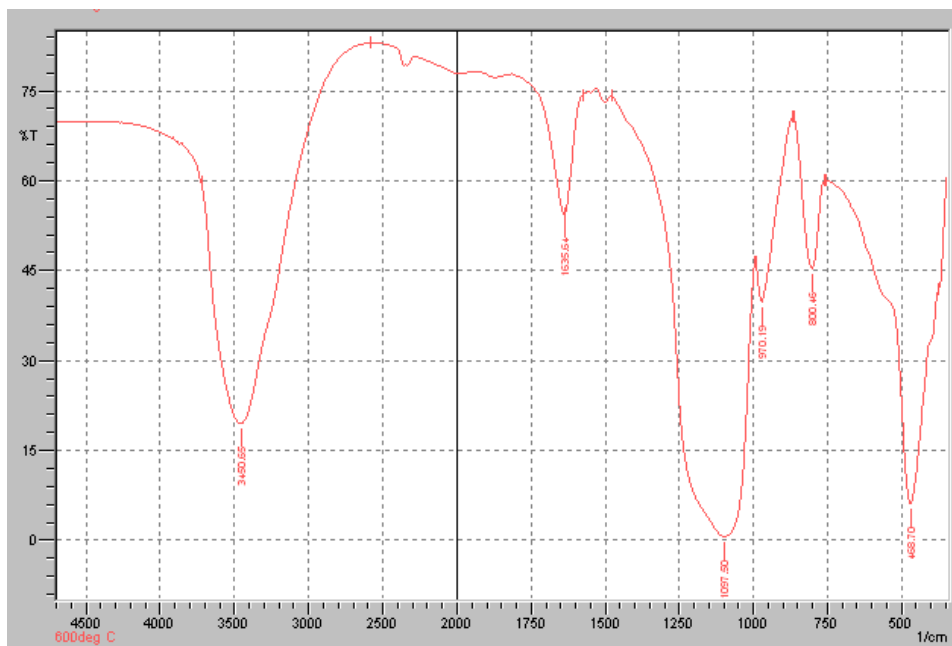


Fig. 7 (b) Co-ferrite silica matrix heated at 600°C

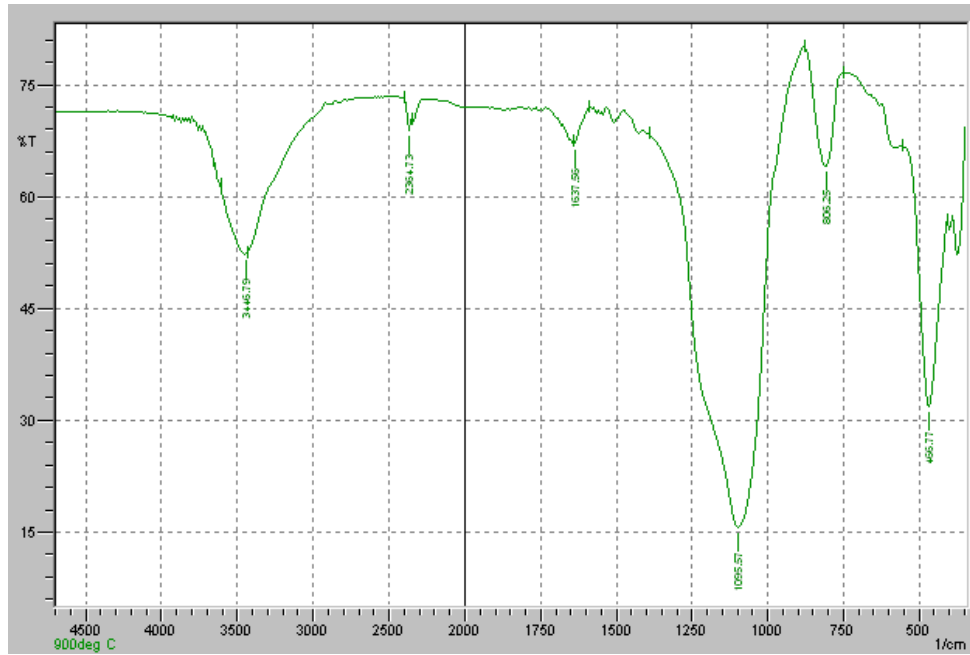


Fig. 7 (c) Co-ferrite silica matrix heated at 900°C

Particle and Crystallite size measurement:

Particle size of silica coated CoFe_2O_4 nanoparticle was measured by nano particle size analyzer which has been shown in Fig. 8 (a). The curve shows the bimodal distribution of particle size. Smaller particles were in range of 18 to 25 nm whereas the bigger particles were from 50 to 300 nm.

X-ray diffraction patterns in Fig. 8(b), of $\text{CoFe}_2\text{O}_4/\text{SiO}_2$ nano-composites shows the amorphous characteristics changed into crystallinity by increasing the temperature. Crystallite sizes of CoFe_2O_4 nano-particle were determined by using Scherer formulae, $t = 0.9\lambda/\beta \cos \theta$. Where, t = Crystallite size; λ = Wavelength (\AA); β = Full width half maximum (FWHM), θ = Bragg's angle Table 1 shows the crystallite size of CoFe_2O_4 . X-ray diffraction patterns for heat treated $\text{CoFe}_2\text{O}_4/\text{SiO}_2$ nano-composites with different CoFe_2O_4 molar concentrations are presented in Fig. 8 (c). By increasing the molar concentration of CoFe_2O_4 , the crystallite size increased [38].

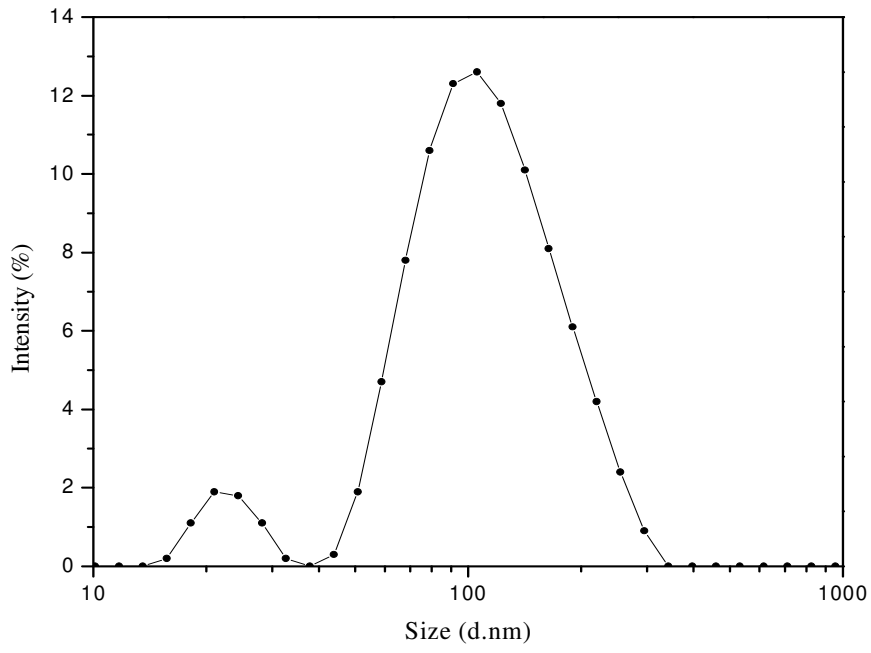


Fig. 8(a) Particle size distribution of silica coated Co-ferrite.

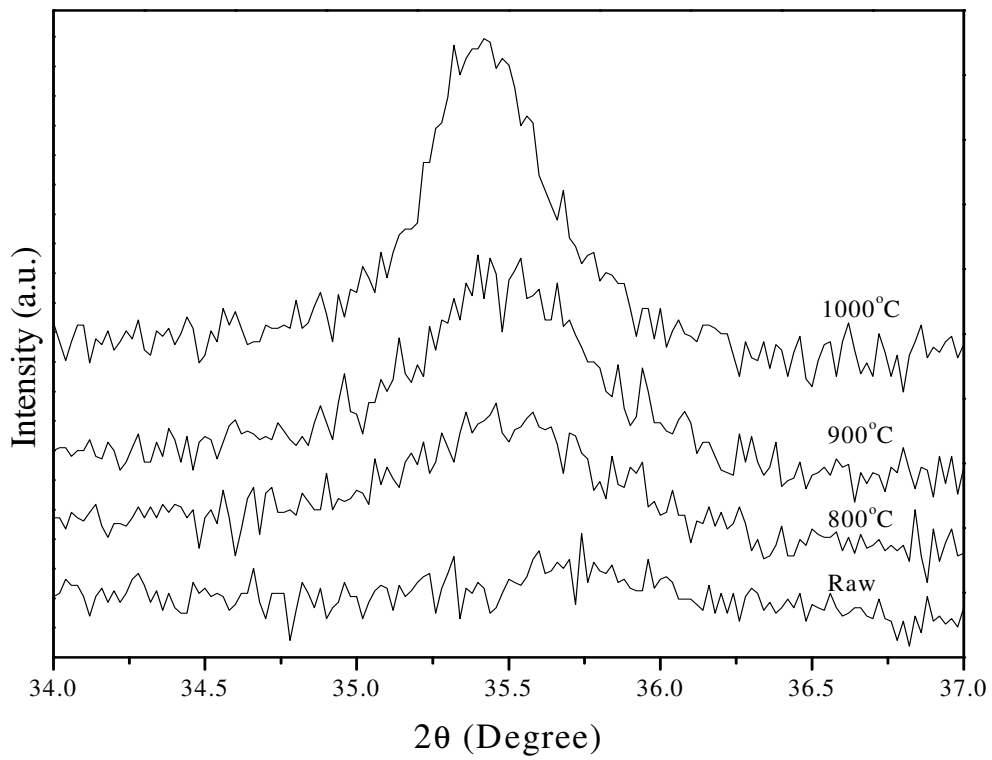


Fig. 8 (b) XRD patterns of the Co-ferrite hosted in silica xerogel

Table 1 Crystallite sizes of CoFe_2O_4 hosted in silica matrix.

Sample	Crystallite Size (nm)
$\text{CoFe}_2\text{O}_4/\text{SiO}_2$ heated at 800°C	27.88
$\text{CoFe}_2\text{O}_4/\text{SiO}_2$ heated at 900°C	30.44
$\text{CoFe}_2\text{O}_4/\text{SiO}_2$ heated at 1000°C	33.57

Crystallite size of Co-ferrite silica matrix samples increased with increasing the number of dipping times; though all the samples were calcined at temperature 1000°C . On increasing the dipping times of silica gel into Co-Fe-nitrate solution, it can be ascribed to the enhanced interactions between the CoFe_2O_4 clusters and silica matrix; hence the crystallite size increased as shown in Fig. 8 (b).

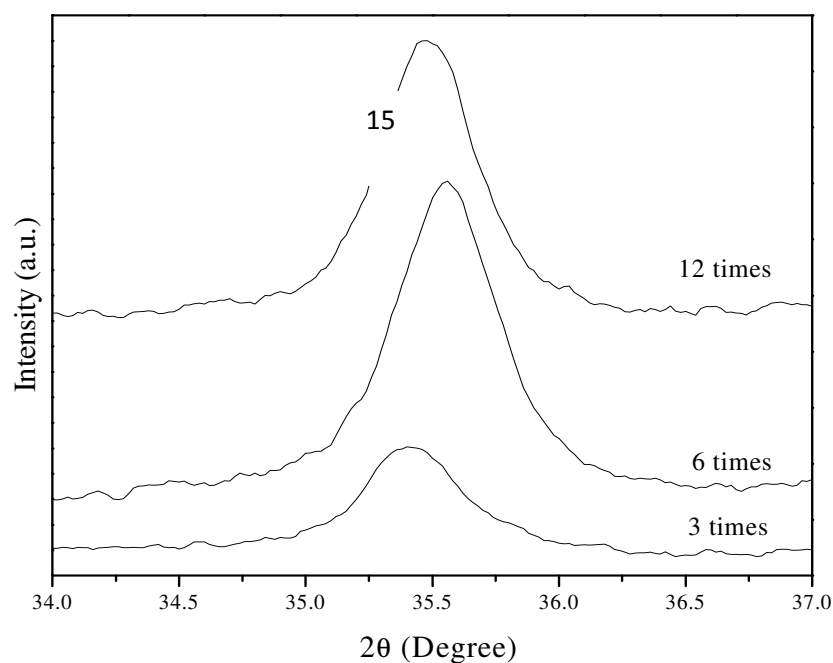


Fig. 8 (c) XRD patterns of the Co-ferrite silica matrix samples prepared by dipping the gel with different times in Co-Fe solution, calcined at 1000°C temperature.

Magnetic Property:

The hysteresis loops of the nanocomposites were collected at RT (Fig 9). M_s values at room temperature were obtained by extrapolation to infinite field in M versus $1/H_2$ plot. The increase in the density of magnetization with the increase in the Fe/Si molar concentration can be observed very clearly. The changes in the magnetic properties of the Nanocomposites can be accounted for by the modification of the average size of nanocrystallites with the Fe/Si molar concentration. The magnetic behavior of this sample is caused by its small crystallite size as revealed by XRD characterization. M_s increases with the increasing of the diameters of CoFe_2O_4 nanocrystallites and its maximum value is 16.6 emu g^{-1} . Considering only the ferrite mass and assuming that the final composition was equal to that of the as-prepared gel, the maximum value of density of magnetization is about 55 emu g^{-1} . The density of magnetization is lower than the reported values for bulk cobalt ferrite (80 emu g^{-1}) [2], but it is in fairly good agreement with the values measured in CoFe_2O_4 particles of similar size. The decrease in the density of magnetization with the decrease in the average diameter of the nanocrystallites can be attributed to surface effects and core-shell morphology. The surface effects are the result of finite-size scaling of nanocrystallites, which in turn leads to a non-collinearity of magnetic moments on their surface. These effects are more intense in ferromagnetic system, where the exchange interaction occurs through the oxygen ion O_2^- (superexchange). The absence of the oxygen ion at the surface or the presence of another atom (ion) in the form of an impurity leads to a break of the superexchange bonds between the magnetic cations which induce surface spin disorder. Due to the above-mentioned effects, the density of magnetization in the nanocrystallites is lower than that of bulk cobalt ferrite. The decrease is more pronounced with the increase in the surface–volume ratio of the nanocrystallites and the decrease in the average diameter of nanocrystallites, respectively. The observed behavior is conditioned by the magnetic structure that corresponds to a single-domain configuration of the crystallites. The maximum value of H_c is as high as 2000 Oe , which is much higher than the coercivity of bulk cobalt ferrite.

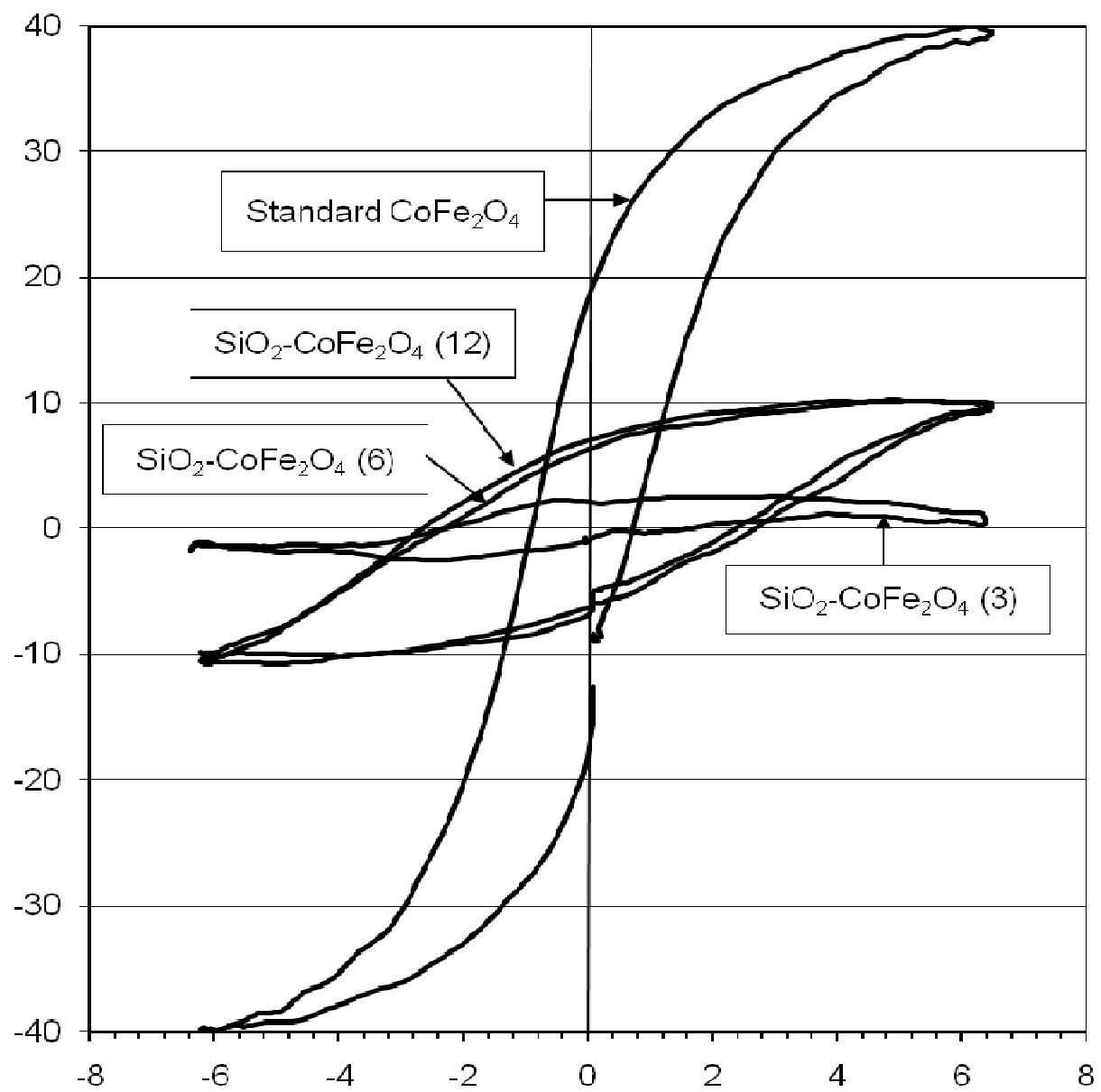
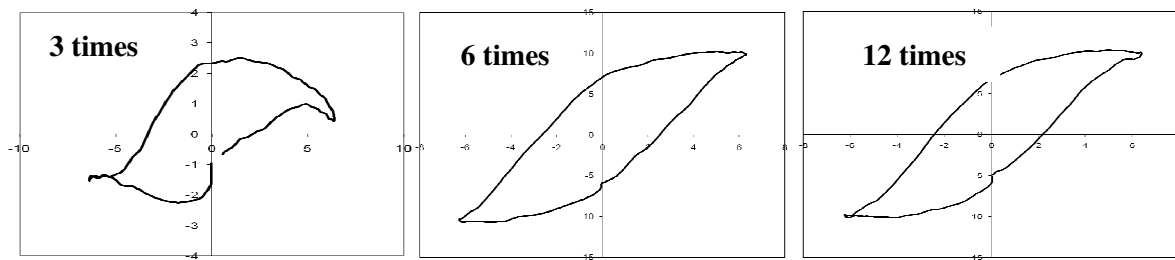


Fig. 9 Magnetization curves for $\text{SiO}_2 / \text{CoFe}_2\text{O}_4$ composite with different molar concentration of CoFe_2O_4 .

Conclusion

CoFe₂O₄/SiO₂ nano-composites were synthesized by a simple processing and subsequently thermal treatment. A wide range of cobalt ferrite particle sizes within the nanometer scale is obtained by this method. By changing the concentration of nitrate salts, particles with an average diameter of 22 nm can be prepared. The magnetic properties exhibit a strong dependence on the crystalline size; Ms values increase with the increase in crystalline sizes ranging from 1.21 to 16.6 emu gK⁻¹. The maximum value of Hc is as high as 2000 Oe, which is much higher than the coercivity of bulk cobalt ferrite.

References

- [1] G.W. Day, A.H. Rose, Proc. SPIE 985 (1988) 138.
- [2] J.I. Mrtin, J. Nogues, K. Liu, J.L. Vicent, I.K. Schuller, J. Magn. Magn. Mater. 256 (2003) 449.
- [3] G.E. Leno, C. Pinyan, Laser FocusWorld 31 (1995) 125.
- [4] U. Hafeli, W. Schutt, J. Teller, M. Zborowski (Eds.), Scientific Clinical Applications of Magnetic Carriers, Plenum Press, New York, 1997.
- [5] D. Shao, A. Xia, J. Hu, C. Wang, W. Yu, Colloids Surf. A 322 (2008) 61.
- [6] G.D. Moeser, K.A. Roach, W.H. Green, P.E. Laibinis, T.A. Hatton, Ind. Eng. Chem. Res. 41 (2002) 4739.
- [7] A. Ditsch, S. Lindenmann, P.E. Laibinis, D.I.C. Wang, T.A. Hatton, Ind. Eng. Chem. Res. 44 (2005) 6824.
- [8] D. Vollath, D.V. Szabo, J. Nanoparticle Res. 1 (1999) 235.
- [9] V.M. Petrov, V.V. Gagulin, Inorg. Mater. 37 (2001) 135.
- [10] F. Mazaleyrat, L.K. Varga, J. Magn. Magn. Mater. 215/216 (2000) 253.
- [11] V. Salgueirino-Maceira, Spasova, M. Farle, Adv. Funct. Mater. 15 (2005) 1036.
- [12] Y. Zhao, C. Ni, D. Kruczynski, X. Zhang, Q.X. John, J. Phys. Chem. B 108 (2004) 3691.
- [13] N.J. Tang, W. Zhong, X.L. Wu, H.Y. Jinag, W. Liu, Y.W. Du, Mater. Lett. 59 (2005) 1723.
- 14. J. Guo, W. Yang, Y. Deng, C. Wang, S. Fu, Small 1, 737 (2005)
- [15] K. Raj, R. Moskowitz, R. Casciari, J. Magn. Magn. Mater. 149 (1995) 174.
- [16] U. Haefeli, W. Schuett, J. Teller, M. Zborowski (Eds.), Scientific and Clinical Applications of Magnetic Carriers, Plenum, New York, 1997.
- [17] M.H. Kryder, MRS Bull. 21 (1996) 17.

- [18] S. Ammar, A. Helfen, N. Jouini, F. Fievet, I. Rosenman, F. Villain, P. Molinie, M. Danot, J. Mater. Chem. 11 (2001) 186.
- [19] H.W. Wang, S.C. Kung, J. Magn. Magn. Mater. 270 (2004) 230.
- [20] S.D. Sartale, G.D. Bagde, C.D. Lokhande, M.G. Iersig, Appl. Surf. Sci. 182 (2001) 366.
- [21] V. Uskokovic, M. Drofenik, Colloids Surf. A 266 (2005) 168.
- [22] A. Verma, T.C. Goel, R.G. Mendiratta, J. Magn. Magn. Mater. 210 (2000) 274.
- [23] E.H. Kim, H.S. Lee, B.K. Kwak, B.K. Kim, J. Magn. Magn. Mater. 289 (2005) 328.
- [24] J.H. Paterson, R. Devine, A.D.R. Phelps, J. Magn. Magn. Mater. 196–197 (1999) 394.
- [25] K.I. Arshak, A. Ajina, D. Egan, Microelectron. J. 32 (2001) 113.
- [26] N.A. Grigorieva, S.V. Grigoriev, A.I. Okorokov, H. Eckerlebe, A.A. Elisrrv, A.V. Lukashin, K.S. Napolskii, Physica E 28 (2005) 286.
- [27] S.M. Prokes, W.E. Carlos, S. Lenward, L. Stephen, G. James L, Mater. Lett. 54 (2002) 85.
- [28] F. Bentivegna, M. Nyvit, J. Appl. Phys. 85 (1999) 2270.
- [29] A.B. Fuertes, J. Phys. Chem. Sol. 66 (2005) 741.
- [30] M. Schwickardi, T. Johann, W. Schmidt, F. Schu" th, Chem. Mater. 14 (2002) 3913.
- [31] T. Valde´s-Solı´s, G.Marban, A.B. Fuertes, Chem.Mater. 17 (2005) 1919.
- [32] M. Schwickardi, T. Johann, W. Schmidt, O. Busch, F. Schuth, Study Surf. Sci. Catal. 143 (2002) 93.
- [33] S.C. Laha, R. Ryoo, Chem. Commun. (2003) 2138.
- [34] B.Z. Tian et al., J. Am. Chem. Soc. 126 (2004) 865.
- [35] B.Z. Tian et al., Adv. Mater. 15 (2003) 1370.
- [36] Y. Men et al., Appl. Catal. A: Gen. 277 (2004) 83.

[37] Y.Q. Wang et al., *Adv. Mater.* 17 (2005) 53.

[38] Shun Hua Xiao, Hai Jun Xu, Jin Hu, Long Yu Li, Xin Jian Li, *Physica E* 40 (2008) 3064–067)